ELSEVIER

Diamond and Related Materials 11 (2002) 301–306

DIAMOND AND RELATED MATERIALS

www.elsevier.com/locate/diamond

In situ plasma diagnostics of the chemistry behind sulfur doping of CVD diamond films

J.R. Petherbridge, P.W. May*, G.M. Fuge, K.N. Rosser, M.N.R. Ashfold

School of Chemistry, University of Bristol, Bristol BS8 1TS, UK

Abstract

Microwave plasma enhanced chemical vapour deposition (CVD) has been used to grow sulfur doped diamond films using a 1% CH_4/H_2 gas mixture with various levels of H_2S addition (100–5000 ppm), upon undoped Si substrates. X-Ray photoelectron spectroscopy has shown that S is incorporated into the diamond at number densities ($\leq$0.2%) that are directly proportional to the H_2S concentration in the gas phase. Four-point probe measurements showed the resistivity of these S-doped films to be a factor of three lower than undoped diamond grown under similar conditions. Sulfur containing diamond film was also obtained using a 0.5% CS_2/H_2 gas mixture, although the high resistivity of the sample indicated that the sulfur had been incorporated into the diamond lattice in a different manner compared with the H_2S grown samples. Molecular beam mass spectrometry has been used to measure simultaneously the concentrations of the dominant gas phase species present during growth, for a wide range of H_2S doping levels (1000–10 000 ppm in the gas phase). CS and CS_2 have been detected in significant concentrations in the plasma region as a result of gas phase reactions. Additional measurements from a 1% CS_2/H_2 plasma gave similar species mole fractions except that no CS was detected. These results suggest that CS may be the first step toward C–S bond formation in the film and thereby a pathway allowing S incorporation into diamond. Optical emission spectroscopy has shown the presence of S_2 in both gas mixtures, consistent with the observed deposition of sulfur on the cool chamber walls.

Keywords: Sulfur doping; In situ diagnostics; Mass spectrometry; Optical emission spectrometry

1. Introduction

The many extreme physical and mechanical properties [1,2] of thin diamond films grown by chemical vapour deposition (CVD) have prompted interest in such films for use in electronic devices. CVD diamond films which exhibit p-type semiconductor properties are routinely grown by addition of B-containing gases such as diborane to the standard CVD gas mixture (1% CH_4/H_2) [3]. Such films find use as electrodes for harsh electrochemical applications (e.g. highly acidic solutions) [4] and in UV detectors [5]. However, obtaining n-type semiconducting diamond films by CVD has proved more challenging, mainly due to the fact that potential donor atoms (e.g. P, O and As) are larger than carbon, discouraging incorporation into the diamond lattice. Although nitrogen readily incorporates into CVD diamond films during growth, the resulting donor levels are too deep (1.7 eV) for many electronic applications [6]. Phosphorus doped diamond films with n-type semiconductor properties have been grown [7], but these exhibit poor crystal quality and conductivity making them unsuitable for some device applications [8]. However, sulfur ion implantation in CVD homoepitaxial diamond (100) films has been reported by Hasegawa et al. [9] to yield films with n-type conductivity, although the results of Hall effect measurements were not conclusive.

Sakaguchi and co-workers [10–12] recently reported that H_2S addition to a 1% CH_4/H_2 gas mixture during microwave plasma enhanced CVD (MPCVD) leads to

*Corresponding author. School of Chemistry, University of Bristol, Cantock's Close, Bristol BS8 1TS, UK. Tel.: +44-117-928-9927; fax: +44-117-925-1295.

E-mail address: paul.may@bris.ac.uk (P.W. May).

0925-9635/02/$ - see front matter
PII: S0925-9635(01)00576-3

the growth of semiconducting, homoepitaxial diamond films exhibiting n-type behaviour. Small H_2S additions ($\sim$100 ppm) were found to improve crystallinity, whereas further increases in H_2S concentrations caused a reduction in crystallinity. Film growth rate was also observed to decline with increased H_2S addition, however the quality of the films (as assessed via Raman spectroscopy) was found to be relatively insensitive to changes in H_2S addition. Relatively high Hall mobilities (597 $cm^2\ V^{-1}\ s^{-1}$) were measured [10] for films produced using H_2S doping levels of 50–100 ppm. However, more recent re-analysis of these samples [13] found that the films exhibited p-type, rather than n-type, semiconducting properties, suggesting that the increased conductivity was due to the presence of boron impurities within the film. Clearly, there remains some uncertainty regarding the ability of H_2S doping to produce n-type conducting CVD diamond.

Studies of the gas phase chemistry leading to deposition of n-type doped CVD diamond films remain rare. Dandy [14] presented thermodynamic equilibrium calculations for $H_2S/CH_4/H_2$ gas mixtures, and concluded that the sulfur precursor dopant species was most probably the SH radical. Experimental measurements of gas phase species concentrations present during the growth of sulfur doped CVD diamond films from H_2S have yet to be reported, however. Molecular beam mass spectroscopy (MBMS) is a powerful technique for carrying out such measurements. Hsu [15] pioneered the use of MBMS to investigate diamond CVD using CH_4/H_2 microwave (MW) plasmas. Gas in that experiment was sampled via an orifice in the substrate, allowing analysis of the composition of the flux incident to the diamond growth surface. Later studies in our group used MBMS to sample gas directly from the plasma, thus probing the gas phase chemistry, with minimum perturbation from gas–surface reactions. This powerful technique has been used to obtain absolute mole fractions of the gas phase species present in a variety of gas mixtures, with and without dopant gas additions, in both hot filament [16–19] and microwave systems [20–22]. Here we report the results of in situ MBMS measurements of species mole fractions, both as a function of input gas composition for H_2S/1% CH_4/H_2 mixtures, and as a function of applied microwave power for a 1% CS_2/H_2 gas mixture. Optical emission spectroscopy has been used in the past to probe the plasma chemistry in a number of gas mixtures, including CH_4/H_2 [23], $O_2/CH_4/H_2$ [24] and CO_2/CH_4 [25,26]; this technique has here been applied to both 1% H_2S/1% CH_4/H_2 and 0.75% CS_2/H_2 gas mixtures.

2. Experimental

2.1. Film deposition

Diamond films were deposited using a 1.5-kW ASTeX-style 2.45-GHz microwave plasma CVD reactor with a water-cooled double-walled chamber containing a Mo substrate holder. This Mo was covered with a Si wafer to prevent the Mo acting as a possible sink for S species (since hot Mo readily reacts with S species to form MoS_2). Undoped Si substrates were placed on an alumina plate and thereby raised $\sim$1 mm into the plasma, with the result that the substrate attained a temperature of $\sim$900 °C, as measured by two colour optical pyrometry. Deposition lasted 8 h with a chamber pressure of 40 torr and applied microwave power of 1 kW. The feedstock gases used were H_2, CH_4 (both with 99.999% purity), and H_2S (99.5% purity). To obtain gas phase H_2S levels below 1000 ppm, a cylinder of 1% H_2S in H_2 was employed and diluted further using appropriate flow ratios regulated by mass flow controllers. Experiments were also performed using a 0.5% CS_2/H_2 gas mixture (using the vapour pressure above a liquid sample of CS_2). Total gas flow for all deposition experiments was 200 sccm.

It is important to stress that this microwave reactor has never been used for processing boron-containing samples, nor had any B-containing gases ever been introduced into it. The chamber was hence completely B free, therefore removing the chance of accidental B-contamination of the samples.

2.2. Film analysis

Films were examined using scanning electron microscopy (SEM) to determine film thickness and crystal morphology, by 514.5 nm (Ar^+) laser Raman spectroscopy (LRS) to assess film quality, and by X-ray photoelectron spectroscopy, XPS, (Mg K_α excitation) to measure sulfur content with a detection limit of $\sim$1000 ppm. The absolute values for the sulfur content (i.e. the S:C number ratio) of the films was calculated by comparing the areas of selected S peak(s) and C peak(s), following calibration using sensitivity factors appropriate for each element. Films were also analysed by secondary ion mass spectrometry (SIMS) [27] to check for impurities (e.g. boron) which might affect the electrical properties of the film (detection limit $\sim$1 ppm). Film resistivity was measured via four-point probe methods [28] at room temperature. Hall effect measurements were made at room temperature with applied magnetic fields up to 2.3 T.

2.3. Optical emission spectroscopy

Optical emission spectra were obtained using an Oriel InstaSpec IV spectrometer to disperse emission from the plasma after exiting through a quartz view port, focusing and passage through a quartz fibre-optic bundle [26]. Light was sampled from the centre of the plasma ball with a spatial resolution of $\sim$3 mm, and a spectral resolution $\leq$0.3 nm, over the wavelength range of 200–

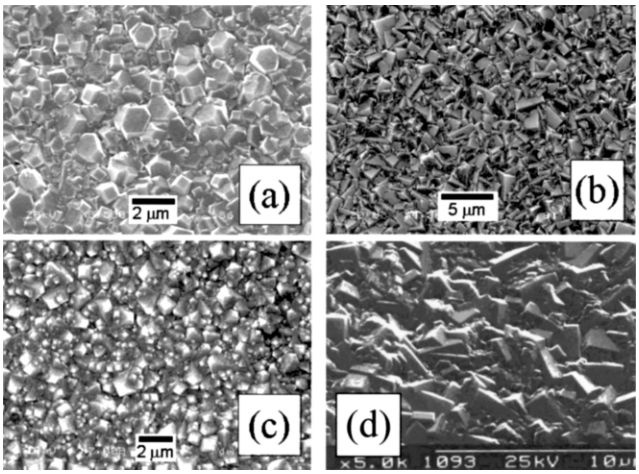

Fig. 1. SEM micrographs for films grown using H_2S additions of (a) 100, (b) 1000 and (c) 5000 ppm to a 1% CH_4/H_2 MW plasma and (d) film growth from a 0.5% CS_2/H_2 MW plasma. Conditions: total gas flow, 200 sccm; growth time, 8 h; substrate temperature, 900 °C; pressure, 40 torr (MW); 1-kW applied microwave power.

520 nm. Spectra obtained for the 1% H_2S/1% CH_4/H_2 and 0.75% CS_2/H_2 gas mixtures were ratioed against a background spectrum recorded using a 100% H_2 mixture in order to highlight effects of H_2S or CS_2 addition.

2.4. Molecular beam mass spectrometry

A full description of the MBMS system and gas sampling technique has been published previously [20]. Sampled species are ionised in the source region of the mass spectrometer by electron impact with the electron ionisation energy user-selectable in the range of 4–70 eV. The electron ioniser energies used to detect species of current interest were: H_2, CH_4 and CS_2 16.0 eV; C_2H_2 13.2 eV (to preclude signal due to the cracking of C_2H_4 occurring above 13.5 eV); H_2S 13.2 eV; CS 13.6 eV (to minimise signal from CO_2 occurring above 13.8 eV) and CH_3 13.6 eV (to reduce signal from cracking of CH_4 above 14.3 eV).

Two sets of species mole fractions were measured. Firstly, H_2S (0–10 000 ppm) was added to a 1% CH_4/H_2 gas mixture maintaining the MW power constant at 1 kW. Secondly, a 1% CS_2/H_2 mixture was introduced into the chamber, and the applied MW power was varied. The chamber pressure for all MBMS experiments was 20 torr and, in each case, the sampling orifice was positioned at the same radial distance from the centre of the MW plasma ball as the substrate during deposition. The correction and calibration procedures applied are as used in previous MBMS studies [16–21].

3. Results

3.1. Film deposition results

Fig. 1a–c shows that there is a marked variation in film morphology with increased H_2S input level. Raising the H_2S input level from 100 to 1000 ppm (Fig. 1a,b) enhances the proportion of (100) oriented facets but further increases (to 5000 ppm, Fig. 1c) results in facets with more rounded forms. Additions of >1000 ppm H_2S to the plasma were also observed to cause deposition of a layer ($\sim$0.5 mm thick after a few hours) of yellow powdery sulfur on the colder parts of the chamber (e.g. the walls and windows).

Fig. 2a shows a gradual fall in film growth rates with increased H_2S levels, consistent with observations made by others [12]. The qualities of the diamond films were measured by LRS, and are presented in Fig. 2b(i). In this case film quality (i.e. the ratio of sp^3:sp^2 carbon bonding) is estimated by comparing the height of the diamond peak at 1332 cm^{-1}, $H(d)$, to that of the graphite feature at 1550 cm^{-1}, $H(g)$. Both intensities are defined relative to an (estimated) underlying spectral background attributed to photoluminescence [29]. Fig. 2b(i) illustrates the progressive decline in film quality seen with increased H_2S addition, although we note that even the most highly doped sample (grown at a S/C input ratio of 0.5) is of good quality, as indicated by the prominent Raman peak at 1332 cm^{-1} [see Fig. 2b(ii)].

Fig. 2c(i) shows the results of XPS analysis of the films. Films deposited with <100 ppm H_2S in the gas mixture showed no S incorporation (below the XPS detection limit) but thereafter the %S detected in the films was found to increase linearly with increased H_2S/CH_4 in the input gas mixture. Note that the incorporation efficiency even at the higher gas phase H_2S levels is still comparatively low (the S/C ratio in the deposited films is only $\sim 1/200$ of that in the input gas mixture). Neither XPS nor SIMS revealed any indication of contamination by B or other unexpected n- or p-dopant atoms. We note that XPS averages the signal over the whole area of the substrate (1 cm^2), and so the position of the S within the film cannot be determined. Depth profiling shows that the S is uniformly distributed throughout the film depth, and not just at the surface, but the spatial resolution of the technique is insufficient to determine if the S is concentrated in say, grain boundaries.

Four-point probe measurements at room temperature show a clear drop in resistivity between undoped (744 Ω-cm) and doped samples (100 and 1000 ppm H_2S, $\sim$200 Ω-cm), as illustrated in Fig. 2c(ii). Unfortunately, due to the high resistivity of these films, measurements of Hall voltage resulted in values below the noise level of the experiment. Therefore, the observed small drop in resistivity may simply reflect the increasing number of grain boundaries and sp^2 carbon content with increasing H_2S addition, rather than any true doping effect.

One film was also deposited on Si using a 0.5% CS_2/H_2 gas mixture. This film exhibited good crystallinity (see Fig. 1d) and gave a clear diamond Raman

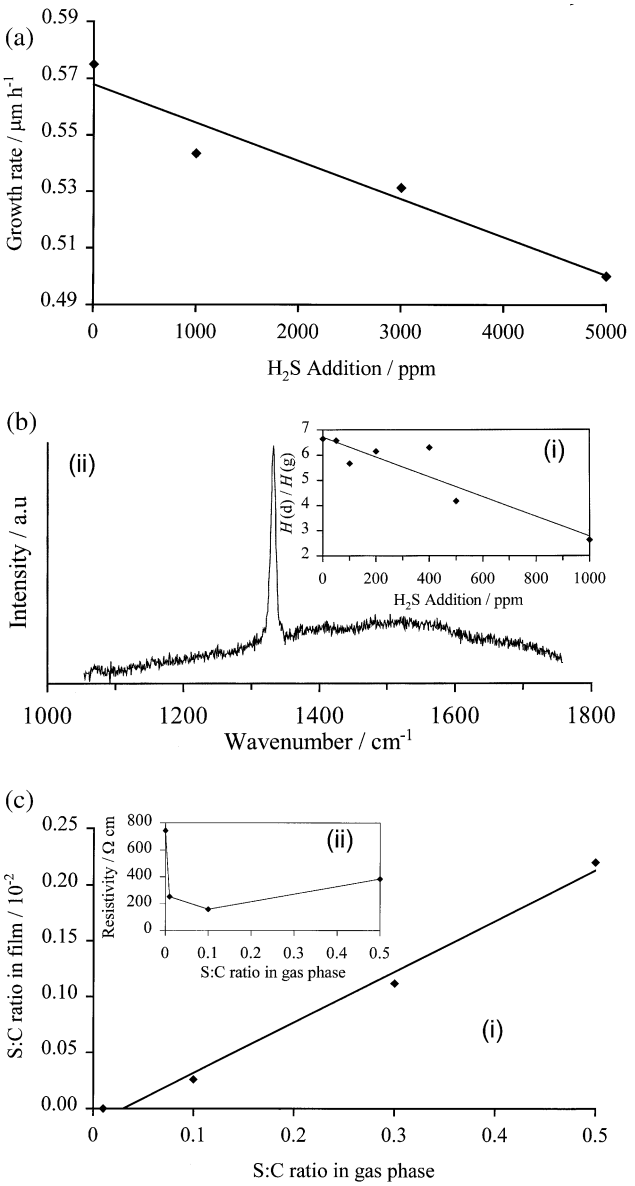

Fig. 2. Plots of (a) film growth rate (measured by cross-sectional SEM) vs. H_2S addition for films grown in $H_2S/1\%\ CH_4/H_2$ gas mixtures. (b)(i) Film quality; and (ii) an example laser Raman spectrum (514.5 nm excitation) for a sample grown using a $0.5\%\ H_2S/1\%\ CH_4/H_2$ gas mixture. Film quality is defined as the ratio of the height of the diamond peak at 1332 cm^{-1}, H(d), to the height of the graphite band at 1550 cm^{-1}, H(g), with both heights are measured relative to an (estimated) underlying spectral background attributed to photoluminescence. (c) Plots of (i) S content (S/C ratio as measured by XPS); and (ii) four-point probe resistivity values of films vs. H_2S addition to a $1\%\ CH_4/H_2$ MW plasma (again quoted as S/C ratio). Conditions as presented in Fig. 1.

peak at 1332 cm^{-1}. XPS showed the S/C content of the film to be ~0.16% but four-point probe measurements revealed the film to be significantly more resistive than the S-doped samples deposited from $H_2S/1\%\ CH_4/H_2$ gas mixtures, suggesting that, in this case, S had been incorporated into the film in a different form. A layer of S was deposited on the cool chamber walls, similar to that observed in the previous H_2S addition experiments.

3.2. Optical emission spectroscopy

Fig. 3 shows the ratioed emission spectra from (a) a $1\%\ H_2S/1\%\ CH_4/H_2$ vs. that from a 100% H_2 plasma and (b) $0.75\%\ CS_2/H_2$ compared to 100% H_2. Both spectra are dominated by emission in the wavelength range 290–540 nm attributable to electronically excited S_2 ($B^3\Sigma^-$) radicals [30]. The emission is stronger for the CS_2/H_2 mixture, as reflected by the distinct blue colouration of the plasma observed when compared to $H_2S/1\%\ CH_4/H_2$ plasmas, probably due, in part at least, to the higher S content in the former mixture. Weak emissions due to CS are also observed from both plasmas (at ~257 and ~266 nm, associated with the $A^1\Pi-X^1\Sigma^+$ transition [30]).

3.3. Molecular beam mass spectrometry

Fig. 4a shows how the mole fractions of the species: CH_4, CH_3, C_2H_2, H_2S, CS_2 and CS vary with increased H_2S addition (0–10 000 ppm) to a $1\%\ CH_4/H_2$ plasma. CH_4, C_2H_2 and CH_3 are all seen to decline, while CS_2 and CS mole fractions are seen to rise. Presented in Fig. 4b is the dependence of species mole fraction on applied microwave power, for a $1\%\ CS_2/H_2$ gas mixture. Increasing the microwave power, at least over the range illustrated in Fig. 4b, has little effect on the relative concentrations of all species, but, in contrast with the

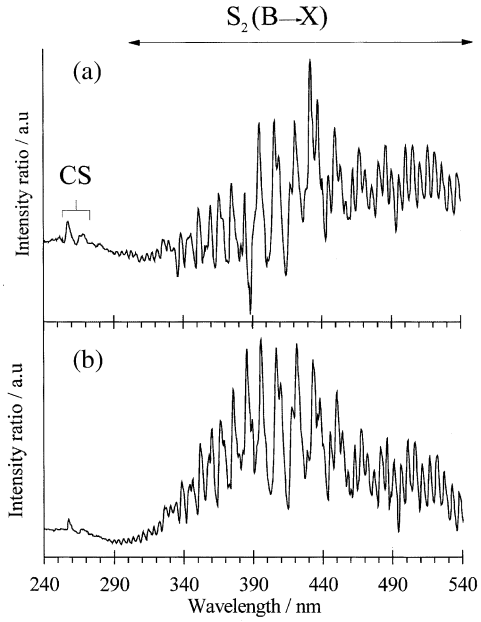

Fig. 3. Ratio plots of (a) $1\%\ H_2S/1\%\ CH_4/H_2$:100% H_2 and (b) $0.75\%\ CS_2/H_2$:100% H_2 optical emission spectra. Conditions: total gas flow, 200 sccm; pressure, 20 torr; 1-kW applied microwave power.

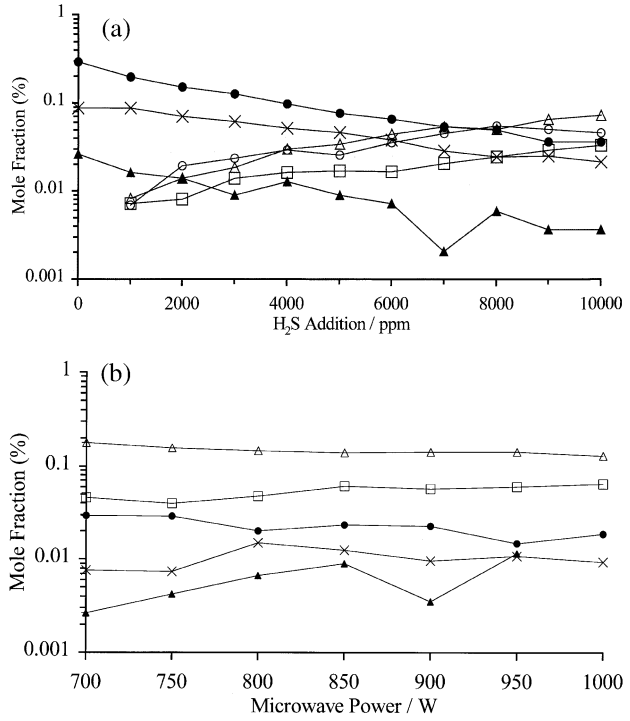

Fig. 4. MBMS results of (a) species mole fraction vs. H_2S addition to a 1% CH_4/H_2 gas mixture and (b) 1% CS_2/H_2 gas mixture measured for various applied microwave powers. Gas was sampled from the edge of the MW plasma ~23 mm from the plasma centre. Conditions: 20 torr, 1-kW applied microwave power. Key: (●) CH_4, (×) C_2H_2, (▲) CH_3, (□) H_2S, (△) CS_2, (○) CS.

$H_2S/1\%$ CH_4/H_2 gas mixtures, no measurable amounts of CS were detected. The CS_2/H_2 plasma was also noted as being significantly larger in size than that for $H_2S/1\%$ CH_4/H_2 gas mixtures (for the same applied microwave power). No detectable levels of SH, S or S_2 were observed in either of the MBMS experiments.

4. Discussion

H_2S addition to 1% CH_4/H_2 MW plasmas allows the incorporation of significant amounts of S (as indicated by XPS) into the CVD diamond film, although (a) the incorporation efficiency is still low (i.e. the S/C ratio in the films is ~1/200 of that in the input gas mixture); and (b) it cannot be determined if the S is concentrated at grain boundaries in these polycrystalline samples. Deposition from a 0.5% CS_2/H_2 MW plasma also yielded a diamond film of good quality, containing sulfur, but with a resistivity significantly greater than that measured for the H_2S grown examples, suggesting that in the case of growth from CS_2/H_2 gas mixtures the S had either been incorporated into the diamond film in a different form, or that it had had less of an effect upon the crystallinity. The observed drop in film growth rates with increased H_2S addition to a 1% CH_4/H_2 gas mixture (Fig. 2a) correlates with the observed drop in CH_3 mole fraction with increased H_2S addition (Fig. 4a), consistent with the assumption that CH_3 is the major diamond growth precursor in low pressure low power CVD reactors [22,31,32].

A detailed model for the gas phase chemistry based upon these observations is presented elsewhere [33] but the main points are summarised here. The dominant overall chemical process for these H/C/S systems is presumed to be Reaction (1), involving the equilibrium between CH_4 and H_2S, and CS_2 and H_2. The Gibbs free energy for this reaction, ΔG_{reac}, is positive at $T<1100$ K, but becomes increasingly negative (i.e. favouring products) as the temperature is increased, reaching -85.0 kJ mol^{-1} at 1600 K.

$$CH_4 + 2H_2S \leftrightharpoons CS_2 + H_2 \qquad \text{Reaction (1).}$$

Reaction (1) as written is, of course, a resultant of many elementary forward and reverse steps in which the chemistry is initiated by H-abstraction from CH_4 and H_2S to form CH_3, SH and H_2. The resulting CH_3 and SH radicals can combine in the presence of a third body to form CH_3SH, which can then undergo successive H-abstraction reactions to yield CS. Further reaction with SH can result in the formation of CS_2.

Fig. 4b illustrates the operation of the reverse of Reaction (1) in which CS_2 and H_2 are converted to H_2S and CH_4, in the cooler regions of the reactor where both H_2 and CS_2 concentrations are high (i.e. essentially the input gas mixture). Diffusion of these products into the hotter regions leads to the formation of CH_3 (the diamond growth species), thus allowing the deposition of diamond from such gas mixtures, as demonstrated here and previously [34]. Such transformations within the input gas mixture prior to sampling the hotter regions of the reactor has many analogues with the recently deduced mechanism for CH_3 production from C_2H_2/H_2 gas mixtures [35].

One possible explanation for the deposition of solid sulfur onto the chamber walls when running both $H_2S/1\%$ CH_4/H_2 and CS_2/H_2 plasmas is that a proportion of the SH radicals produced within the plasma diffuse out to the cooler regions of the reactor, where they recombine to form S_2 — some of which is electronically excited and thus detected in the OES spectrum (Fig. 3). The S_2 species then aggregate to form larger S_x clusters, which then deposit as solid S on the chamber walls.

It is interesting to note that, in spite of the high input concentration of CS_2 in the 1% CS_2/H_2 gas mixture, no CS was detected by MBMS (Fig. 4b). The reason for this may be that T_{gas} is lower for the 1% CS_2/H_2 plasma than the $H_2S/1\%$ CH_4/H_2 plasmas. This is suggested by the larger size of the former plasma ball (at a fixed power input) which would result in a lower power density, and thus a lower average temperature, within the plasma. We note, however, that CS was detected by

OES in the 1% CS_2/H_2 plasma, implying that (compared with MBMS) OES is a more sensitive (although not quantitative) detection method for such radical species. Additionally MBMS failed to detect any S_2, whereas OES detected this species in both H_2S/1% CH_4/H_2 and CS_2/H_2 plasmas. As discussed above, S_2 is predicted to form in the cooler regions of the plasma. OES monitors a column of plasma, including the cooler outer parts, whereas the present MBMS arrangement samples gas from deeper into the plasma. It seems likely therefore that the non-observation of S_2 by MBMS reflects the fact that: (a) it is a relatively insensitive technique for short lived radical species; and (b) it is not sampling the plasma in the region where S_2 concentrations are maximal.

In conclusion, detailed investigations of gas composition in both H_2S/1% CH_4/H_2 and CS_2/H_2 MW plasmas using MBMS and OES techniques have provided new insight into the fundamental chemistry occurring in the gas phase. We speculate that CS may well be the dominant species responsible for the inclusion of S into the diamond films.

Acknowledgments

Financial support from the EPSRC and De Beers Industrial Diamond, Ltd is gratefully acknowledged. The authors are also grateful to Sean Pearce, Drs Jason Riley, Dudley Shallcross, Jeremy Harvey, and Jonathan Hayes, Pippa Hawes, and Les Corbin for their many and varied contributions to aspects of this work.

References

[1] K.E. Spear, J.P. Dismukes, Synthetic Diamond, Emerging CVD Science and Technology, Wiley, New York, 1994.
[2] P.W. May, Philos. Trans. R. Soc. Lond., A 358 (2000) 473.
[3] M.N. Latto, D.J. Riley, P.W. May, Diamond Relat. Mater. 9 (2000) 1181.
[4] N. Vinocur, B. Miller, Y. Avyigal, R. Kalish, J. Electrochem. Soc. 143 (1996) L238.
[5] V.I. Polyakov, A.I. Rukovishnikov, N.M. Rossukanyi, et al., Diamond Relat. Mater. 7 (1998) 821.
[6] R.G. Farrer, Solid State Comm. 7 (1969) 685.
[7] S. Koizumi, M. Kamo, Y. Sato, et al., Diamond Relat. Mater. 7 (1998) 540.
[8] S. Bohr, R. Haubner, B. Lux, Diamond Relat. Mater. 4 (1995) 133.
[9] M. Hasegawa, D. Takeuchi, S. Yamanaka, et al., Jpn. J. Appl. Phys. 38 (1999) L1519.
[10] I. Sakaguchi, M.N. Gamo, Y. Kikuchi, E. Yasu, H. Haneda, Phys. Rev. B 60 (1999) R2139.
[11] M.N. Gamo, E. Yasu, C. Xiao, et al., Diamond Relat. Mater. 9 (2000) 941.
[12] M.N. Gamo, C. Xiao, Y. Zhang, et al., Thin Solid Films 382 (2001) 113.
[13] R. Kalish, A. Reznik, C. Uzan-Saguy, C. Cytermann, Appl. Phys. Lett. 76 (2000) 757.
[14] D.S. Dandy, Thin Solid Films 318 (2001) 1.
[15] W.L. Hsu, J. Appl. Phys. 72 (1992) 3102.
[16] C.A. Rego, P.W. May, C.R. Henderson, M.N.R. Ashfold, K.N. Rosser, N.M. Everitt, Diamond Relat. Mater. 4 (1995) 770.
[17] R.S. Tsang, C.A. Rego, P.W. May, et al., Diamond Relat. Mater. 5 (1996) 359.
[18] C.A. Rego, R.S. Tsang, P.W. May, M.N.R. Ashfold, K.N. Rosser, J. Appl. Phys. 79 (1995) 7264.
[19] R.S. Tsang, P.W. May, M.N.R. Ashfold, K.N. Rosser, Diamond Relat. Mater. 7 (1998) 1651.
[20] S.M. Leeds, P.W. May, E. Bartlett, M.N.R. Ashfold, K.N. Rosser, Diamond Relat. Mater. 8 (1999) 1377.
[21] S.M. Leeds, P.W. May, M.N.R. Ashfold, K.N. Rosser, Diamond Relat. Mater. 8 (1999) 226.
[22] J.R. Petherbridge, P.W. May, S.R.J. Pearce, K.N. Rosser, M.N.R. Ashfold, J. Appl. Phys. 89 (2001) 1484.
[23] A. Inspektor, Y. Liou, T. McKenna, R. Messier, Surf. Coat. Technol. 39/40 (1989) 211.
[24] J.A. Mucha, D.L. Flamm, D.E. Ibbotson, J. Appl. Phys. 65 (1989) 3448.
[25] T.P. Mollart, K.L. Lewis, Diamond Relat. Mater. 8 (1999) 236.
[26] M.A. Elliott, P.W. May, J. Petherbridge, S.M. Leeds, M.N.R. Ashfold, W.N. Wang, Diamond Relat. Mater. 9 (2000) 311.
[27] P.E.J. Flewitt, R.K. Wild, Physical Methods of Materials Characterisation, Institute of Physics Publishing, Bristol, 1994.
[28] S.M. Sze, Physics of Semiconductor Devices, Wiley, New York, 1981.
[29] S.M. Leeds, T.J. Davis, P.W. May, C.D.O. Pickard, M.N.R. Ashfold, Diamond. Relat. Mater. 7 (1998) 233.
[30] R.W.B. Pearse, A.G. Gaydon, The Identification of Molecular Spectra, Chapman and Hall, London, 1976.
[31] B.J. Garrison, E.J. Dawnkaski, D. Srivastava, D.W. Brenner, Science 255 (1992) 835.
[32] S.J. Harris, D.G. Goodwin, J. Phys. Chem. 97 (1993) 23.
[33] J.R. Petherbridge, P.W. May, G.M. Fuge, K.N. Rosser, M.N.R. Ashfold, J. Appl. Phys. (in press).
[34] G.D. Barber, W.A. Yarbrough, J. Am. Ceram. Soc. 80 (1997) 1560.
[35] J.A. Smith, E. Cameron, M.N.R. Ashfold, Y.A. Mankelevich, N.V. Suetin, Diamond Relat. Mater. 10 (2001) 358.